SAE INTERNATIONAL

Effect of the Shape of the Combustion Chamber on Dual Fuel Combustion

2013-24-0115
Published
09/08/2013

Teresa Donateo, Luciano Strafella, and Domenico Laforgia
Universita del Salento

doi:10.4271/2013-24-0115

ABSTRACT

The effect of the shape of the bowl on the combustion process and emissions of a Natural Gas - Diesel dual fuel engine is analyzed. The simulation of the dual fuel combustion is performed with a modified version of the KIVA3V code where diesel is treated as the main fuel and a further reacting specie is introduced as methane (CH_4). The auto-ignition of the pilot is simulated with a modified version of the Shell model and the first stage of the combustion, related to the pilot burning process, is simulated with the Characteristic Time Combustion model. When the temperature of the mixture reaches a certain threshold, a kernel of combustion is initialized. Until the kernel reaches a nominal radius the combustion of CH_4 is prevented. The combustion of CH_4 is simulated with a turbulent characteristic time too. Numerical models were chosen as a compromise between accuracy and computational time. The model has been validated with comparison to experimental data including in-cylinder pressure traces and tailpipe emissions. The numerical analysis has been performed with respect to a single cylinder diesel engine converted to dual fuel combustion. The results of the investigation showed that the conversion rate of CH_4 can be increased by optimizing the bowl profile.

INTRODUCTION

Gaseous fuels like natural gas have been extensively investigated in literature [1, 2, 3, 4] as alternative to gasoline and diesel. Compressed Natural Gas (CNG) has higher octane number than gasoline, is more economical than traditional fossil fuels due to its low production cost, and reduces air pollution significantly [2]. Moreover, CNG contains neither lead nor benzene and greenhouse gases emission from combustion of CNG is about 25% lower than that of gasoline. Another important advantage of CNG is the high stability against knocking and the possibility to use higher compression ratios than gasoline engines thus increasing brake thermal efficiency and power [2]. On the other hand, the higher compression ratio causes greater NO_x [2].

Two different methods have been developed to convert a direct injection diesel engine into a natural gas engine, *CNG dedicated* and *Dual Fuel.* In the first case, ignition is performed with the use of a spark plug like in a gasoline engine while the dual-fuel mode uses compressed natural gas (CNG) as the primary fuel and small quantities of diesel pilot-fuel for ignition. Dual-fuel engines deriving from the conversion of conventional diesel engines usually operate un-throttled, with the load regulated by the admission of natural gas in the intake manifold. This introduce a further challenge in the numerical simulation of this systems i.e. the lean fuel combustion mode. Dual fuel engines have lower emissions of smoke and nitrogen oxides than conventional CI engines while maintaining their high thermal efficiencies. However, an increase of emissions of unburned hydrocarbons (HC) and carbon monoxide (CO) is obtained due to poor ignitability of the mixture [4].

In the conversion of a diesel engine to dual fuel, it is important to keep the original components of the engine in order to reduce the conversion costs. However, some alterations have to be made to optimize the behavior of the engine when CNG is used. Direct Injection diesel engines use re-entrant bowl with a central protrusion in order to improve the air-fuel mixing and accelerate the combustion process. Of course, this kind of combustion chamber is not optimized for dual fuel combustion. The aim of the present investigation is to study the effect of the combustion chamber in the diesel-

CNG conversion and optimizing its design with the help of a computer aided procedure already applied to several diesel engine configurations [5,6]. The procedure is based on the coupling of a multi-objective genetic algorithm with a multi-dimension simulation code able to accurately predict the combustion process. The effectiveness of the procedure results have been experimentally verified by building and testing the optimized combustion chamber [5]. The key issue is the validity of the simulation model used to simulate the combustion process.

Dual fuel combustion is extremely complex because it involves two fuels with different characteristics which are simultaneously burned inside the cylinder. The heat release rate of dual fuel combustion is the results [7, 8] of three combustion stages: the combustion of the pilot injection of diesel fuel, the combustion of the gaseous fuel that is in the immediate vicinity of the ignition kernel and the pre-ignition activity and subsequent turbulent flame propagation. However, the relevance of the third stage depends on the amount of natural gas. In the case of very lean mixtures, no consistent flame propagation will take place from the ignition centers and combustion is mainly influenced by the pilot combustion. Only when the mixture becomes richer, a more regular propagation of the flame can be obtained.

Detailed models of dual fuel combustion describe the complex chemical mechanisms that govern the oxidation process. The chemical kinetic schemes involve thousands of elementary reaction steps that are believed to take place in this kind of engines [10]. Since the rate coefficients are determined on the basis of fundamental chemical processes, there should be no need to adjust any of the rate coefficients of the schemes. However, detailed chemical models may need some calibration because the actual kinetic mechanisms for each combustion process are unknown. Moreover, the required computational time is still prohibitive in the case under examination. In fact, the coupling of the CFD model with the multi-objective genetic algorithm require hundreds of runs to be performed with respect to different combustion chamber profiles [5].

Reitz et al. [9, 11] developed a new combustion model for dual fuel engine where flame propagation is simulated with the level set method of Peters [12]. According to the analysis of Reitz et al. [9, 11], ignition occurs in two different positions, namely in the vicinity of the nozzle injector and in the region of the combustion chamber where the spray impacts on the cylinder walls. Then, combustion extends through the remaining part of the chamber, but leaves unburned a large proportion of mixture next to the wall of the cylinder.

The engine models presented in this paper have been chosen as a compromise between accuracy and computational load so to allow the execution of the multi-objective optimization in a reasonable time. The models have been validated through comparison to experimental data on a reference engine. In the present investigation, lean mixtures are considered ($0<ER<0.4$) and dual fuel combustion is modeled with the characteristic time combustion model for both diesel and methane. The advanced models for ignition and spray already implemented in the KivaCREA code have been used [13, 14, 15].

Experimental Tests

The engine considered in the present investigation (Table 1) is a single cylinder optical engine under test at the Department of Engineering for Innovation for the conversion from direct injection diesel combustion to dual fuel mode.

A comprehensive experimental campaign with the experimental layout of Figure 1 has been performed by Carlucci et al. [16] to investigate the effect of the intake valve configurations on the dual fuel combustion.

Although the engine is provided with two intake ducts (see Figure 2), during the experiments only the swirl port was left open. The experimental data presented here include both in-cylinder pressure traces and emissions levels that have been used for the validation of the proposed combustion model.

Table 1. Engine specification

Maximum power	18 kW	
Bore	85 mm	
Stroke	90 mm	
Compression ratio	17,1:1	
Combustion chamber	Bowl with valve pockets and flat head	
Injection system	Common Rail	
Max. Injection pressure	1300 bar	
Number of nozzles	5	
Nozzle diameter	170 μm	
Spray angle	142°	
Valve timing	Opening	Closing
Intake	13.5° BTDC	46.5° ABDC
Exhaust	51.5° BBDC	16.5° ATDC

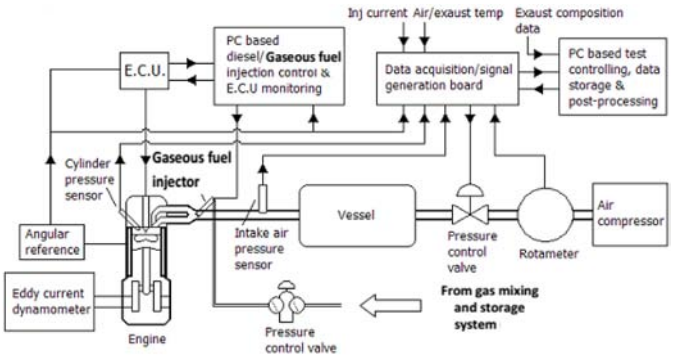

Figure 1. Experimental setup

The gaseous fuel is introduced in the intake duct by means of an injector. The Department of Engineering for Innovation

and in particular the Machinery Laboratory of University of Salento is equipped with a mixing system for gaseous fuels (Figure 3): this system allows to obtain a gaseous mixture of five species (CO_2, CO, H_2, N_2, CH_4) with the opportunity to decide their percentage; the pressure levels of the mixture so obtained can vary in the range 1-10 bar abs, is sent in an accumulation tank and from here to the ICE. In the present investigation pure Methane was considered.

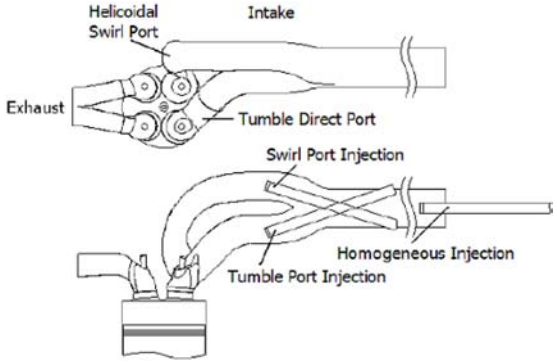

Figure 2. Intake manifold geometries and gaseous fuel injection positions

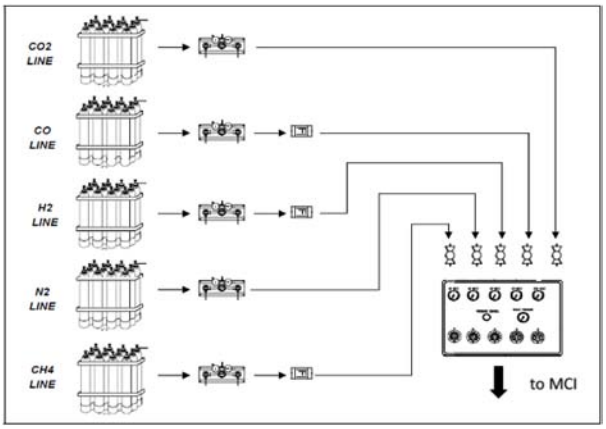

Figure 3. Mixing system for gaseous fuels

The electronic control of the system has been realized through FPGA managed by a LabView® Virtual Instrument. This system generates the signal that controls the solenoid valve by means of the acquisition of two signals from a sensor mounted on the fly-wheel and the other on the pulley fixed on the high pressure pump.In order to obtain a more homogeneous gaseous air-fuel mixture the injector has been positioned along the intake duct to a distance of about 40 cm from the cylinder axis (see Figure 2).In order to ensure that all the gaseous fuel enters the cylinder, gas injection has been modified advancing the angle corresponding to the start of injection while the angle corresponding to the end of the injection has been keep constant and equal to 195 deg BTDC.

Specific tests were executed in order to validate the dual fuel combustion model. In all the tests, the mass of diesel fuel was kept constant to 5.0 mg by considering the same injection pressure (500bar) and the same energizing time (300 ms). The mass in the cylinder was also kept constant by setting the same pressure at Top Dead Center for all the tests without methane.

A first set of tests (Table 2 -Case 1) was performed by changing the advance of the pilot and the engine speed with and without methane. The second set (Table 3 - Case 2) was obtained by changing only the mass of methane.

Table 2. Case 1

Engine speed	Pilot advance	Mass of CH_4	IMEP	ER at IVC
1500 rpm	7.5 BTDC	0	1.43 bar	0
1500 rpm	7.5 BTDC	15 mg	4.83 bar	0.38
1500 rpm	2.5 BTDC	0	1.33 bar	0
1500 rpm	2.5 BTDC	15 mg	4.77 bar	0.38
2000 rpm	2.5 BTDC	0	1.52 bar	0
2000 rpm	2.5 BTDC	15 mg	4.31 bar	0.38

Table 3. Case 2

Engine speed	Pilot advance	Mass of CH_4	IMEP	ER at IVC
1500 rpm	7.5 BTDC	0	1.43 bar	0
1500 rpm	7.5 BTDC	4.3 mg	1.64 bar	0.11
1500 rpm	7.5 BTDC	7.0 mg	2.12 bar	0.18
1500 rpm	7.5 BTDC	15 mg	4.83 bar	0.38

The procedure for the dual fuel tests consists of the following steps:

- set the gas pressure;
- run the engine at the desired speed;
- inject the Diesel fuel with fixed values of q_{pilot}, p_{rail}, SOI_{pilot}
- inject the gaseous fuel (as previously explained) until the desired mass of methane is reached.

The parameters of interest were acquired, as cylinder pressure and pollutant emission levels at the exhaust, by means of an AVL AMA i60 emission analyzer.

Part-load condition and lean mixture have been considered. These operating modes were chosen for the difficulty to guarantee a satisfactory combustion process due to the low amount of methane burnt in this condition. Further investigation will take into account full load conditions where the main challenge is to achieve the same torque curve as the original diesel engine [17].

ENGINE MODELING

A complete fluid-dynamic analysis of the engine should include the intake phase and the closed-valve portion of the cycle. However, according to the simulation of the intake process performed by the authors with the Fluent code, it is possible to simplify the problem.

Open-valves Simulation

Figure 4 shows the distribution of methane (CH_4) at 4°BTDC obtained with the Fluent code run with initial conditions found with the help of 1-D simulation code (AVL-Boost). Note that, even if the charge is stratified at the intake, the mixture is quite homogeneous at the end of the compression stroke before the injection of the diesel fuel. This result shows that the hypothesis of distribution uniformity of the gaseous fuel during the whole compression stroke can be accepted.

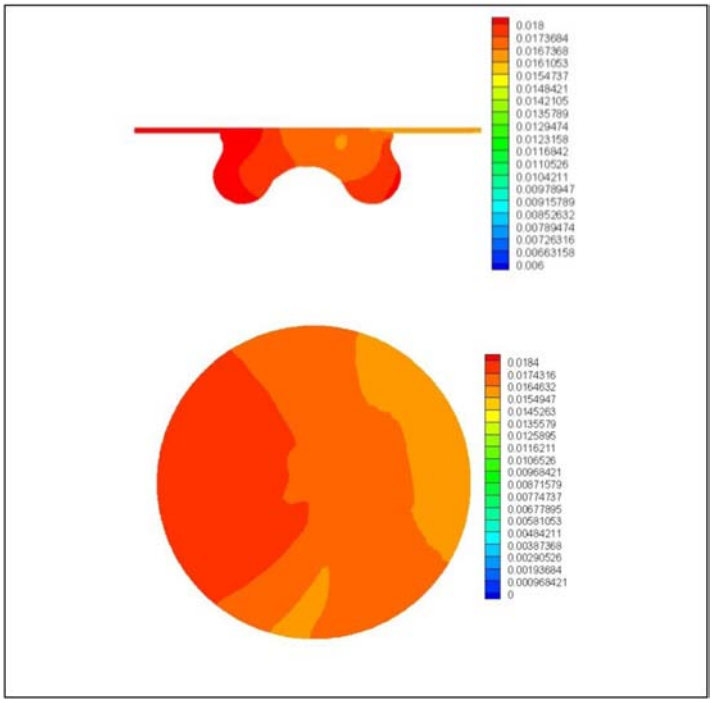

Figure 4. Molar fraction of CH_4 at 4° BTDC calculated with complete 3D simulation

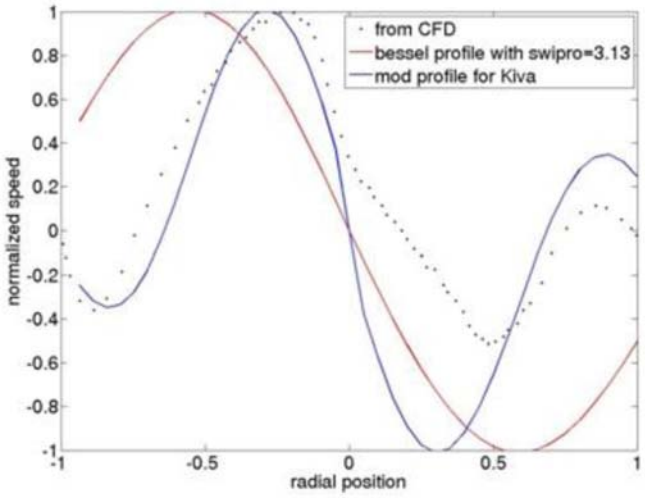

Figure 5. Swirl profile calculated with complete 3D simulation

The results of the 3D complete simulations also include the swirl profile and the specification of the turbulent flow field obtained with the original piston (Figure 5). The swirl profile obtained with the Fluent simulation is represented by the dotted line. Note that it is not axis-symmetrical as assumed in the simulation of the closed-valve phase with the Kiva3v code where the flow field is set at the Intake Valve Closing with a parametric Bessel profile according to the value of a parameter named "*swipro*" (considered equal to 3.13 in Figure 5 as suggested in literature [18]). However, the assumption of symmetry can be important to reduce the computational time. Since diesel fuel is injected with a central five-hole injector, the simulation of a sector of 72° could be performed. To this, a modified profile (blue line) has been considered for the simulations with Kiva3CREA. The modified profile is still symmetrical but more similar to that obtained by the complete simulation. In particular, it captures the inversion of the flow rotation near to the cylinder walls.

Complete simulations with Fluent have been performed also to assess the effect of changing the shape of the bowl on the flow field generated during the intake phase [22]. To this, the original bowl has been replaced with two arbitrary bowls named "Bowl 1" and "Bowl 2". The results of the simulation are reported in Table ***4***. Note that the quantitative parameters and the qualitative distribution of the length scale of turbulence are only weakly affected by the shape of the piston.

According to the results of this analysis, it is reasonable to limit the simulation to the closed-valve portion of the engine cycle if the goal is the optimization of the combustion process by changing the bowl design. Of course, complete 3D simulations would be very useful if the optimization would include the design of the intake manifolds or the valve lift profile.

Table 4. Effect of the bowl profile on the flow field at Intake Valve Closing

	Baseline	Bowl 1	Bowl 2
Global turbulent kinetic energy [m^2/s^2]	22.02	20.14	21.03
Density of turbulent kinetic energy	1.22	1.12	1.17
Swirl speed [rad/s]	269.6	271.4	270.6
Swirl ratio	1.287	1.296	1.292
Length scale of turbulent fluctuations 5.13 E-06 [m] 2.7 E-0.3 [m]	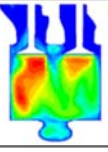	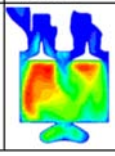	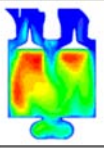

Closed-valves Simulation

In the present work, a modified version of KIVA 3V code developed at the CREA Research Center of University of Salento is used for the close-valve portion of the engine cycle. This version, named Kiva3CREA, was obtained by eliminating the hypotheses of constant fuel density, the constant spray angle and by using an improved version of the Shell model [13,14] that was found to be able to predict the

ignition delay both for very early and very delayed injections and large amount of EGR levels [13]. Some modifications were required to simulate the dual fuel combustion with the KivaCREA. Diesel was treated as the main fuel, thus the spray models for injection, breakup, collisions and evaporation were not modified. The second fuel, CH_4, was treated as a component of the air at the Intake Valve Closing and its properties are calculated with the standard fuel subroutine of Kiva3v.

Combustion and Emissions

The auto-ignition of the pilot is simulated with the modified Shell mode and the first stage of the combustion, related to the pilot burning process, is simulated with the Characteristic Time Combustion model [14]. When the temperature of the mixture reaches 1150K, a kernel of combustion is initialized. Until the kernel reaches a nominal radius the combustion of CH_4 is prevented. The critical radius is calculated as [11]:

$$r_{crit} = 0.32\frac{k^{1.5}}{\varepsilon} \tag{1}$$

Where k is the turbulence kinetic energy and ε is its dissipation rate. Once the kernel is formed, the CH_4 in the proximity of the kernel burns with a conversion rate calculated according to a turbulent combustion time for methane. CH_4 only burn if the mixture temperature is higher a threshold value T_{th} and the equivalence ratio is between the lean and rich limits for methane. The model includes two empirical parameters to match experimental data: the threshold temperature T_{th} and the turbulent time constant called C_3.

$$\tau_{t,CH_4} = C_3\frac{k}{\varepsilon} \tag{2}$$

A new species *phi* that does not participate in the combustion was also introduced to implement the Level Set model and its transport vectors were defined, but the simulations have shown that the species *phi* does not propagate within the chamber in correspondence of lean mixtures. Further investigation are needed. As far as emissions are concerned, the authors have not found in literature a model for dual fuel CNG engines that is able to accurately predict the emissions of CO and HC with acceptable computational times (e.g. without using detailed kinetic schemes). On the other hand, the main trends of NO_x, and soot emissions can be captured with the standard models used for diesel engines [19]. In particular, NO_x emissions can be predicted with the well known Zeldovich Mechanism [19]. In the case of HC, the emissions are evaluated numerically by considering the amount of CH_4 fuel unburned at the end of the simulation. Thus, other causes of unburned hydrocarbons like the lubricant and are not taken into account. For this reason, the numerical value of unburned CH_4 can be considered more as a measure of the completeness of combustion than of the actual HC emissions.

Validation of the Model

The validation was aimed at checking the capability of the simulation code in predicting the effect of increasing the mass of the methane and changing engine speed and pilot advance. The parameters of the spray, ignition and combustion models were set equal to the values of Table 5 and kept constant for all operating conditions. The code was tested over the experimental tests of Case 1 and Case 2 where the engine speed and the pilot advance are changed. The experimental and numerical pressure traces are shown in Figure 6 and Figure 9. The experimental in-cylinder pressure traces are obtained by averaging 100 cycles for each case. However, the cycle-to-cycle dispersion was found to be very high in the tests with >15 mg of CH_4.

Table 5. Tuning of the model

Parameters	Model	Tuning value
Af04	modified shell model [13]	$1.22 \cdot 10^6$
Af0a	modified shell model [13]	$1.01 \cdot 10^9$
B_1	Break-up time constant [18]	40
distant	Break-up time constant [18]	2.0
cm_2	constant for turbulent characteristic time for diesel fuel [18]	0.5
denomc	constant for laminar characteristic time for diesel fuel [18]	1.44
c_3	constant for turbulent characteristic time for CH_4	0.05
T_{th}	threshold temperature for methane combustion	1150K

The ROHR plots represent the apparent net heat release, i.e. the difference between the gross ROHR and the heat transfer rate, calculated by the pressure p measured in the chamber and the swept volume V [19] as:

$$netROHR = \frac{\gamma}{\gamma-1}p\frac{dV}{d\vartheta} + \frac{1}{\gamma-1}V\frac{dp}{d\vartheta} \tag{2}$$

where θ is the crank angle and γ is the ratio between constant pressure and constant volume specific heat of the mixture. The variation of γ with mixture composition [20] and the contribution to net ROHR due to blow-by flows [21] are not taken into account.

Case 1

The experimental and numerical pressure traces are shown in Figure 6. The first row shows the tests with diesel fuel only while the second row describes the results obtained by adding 15 mg of CH_4 per cycle. Note that the numerical code predicts very well the pressure traces in the case of diesel only while underestimates the combustion rate and overestimate the ignition delay in the case with CH_4, thus

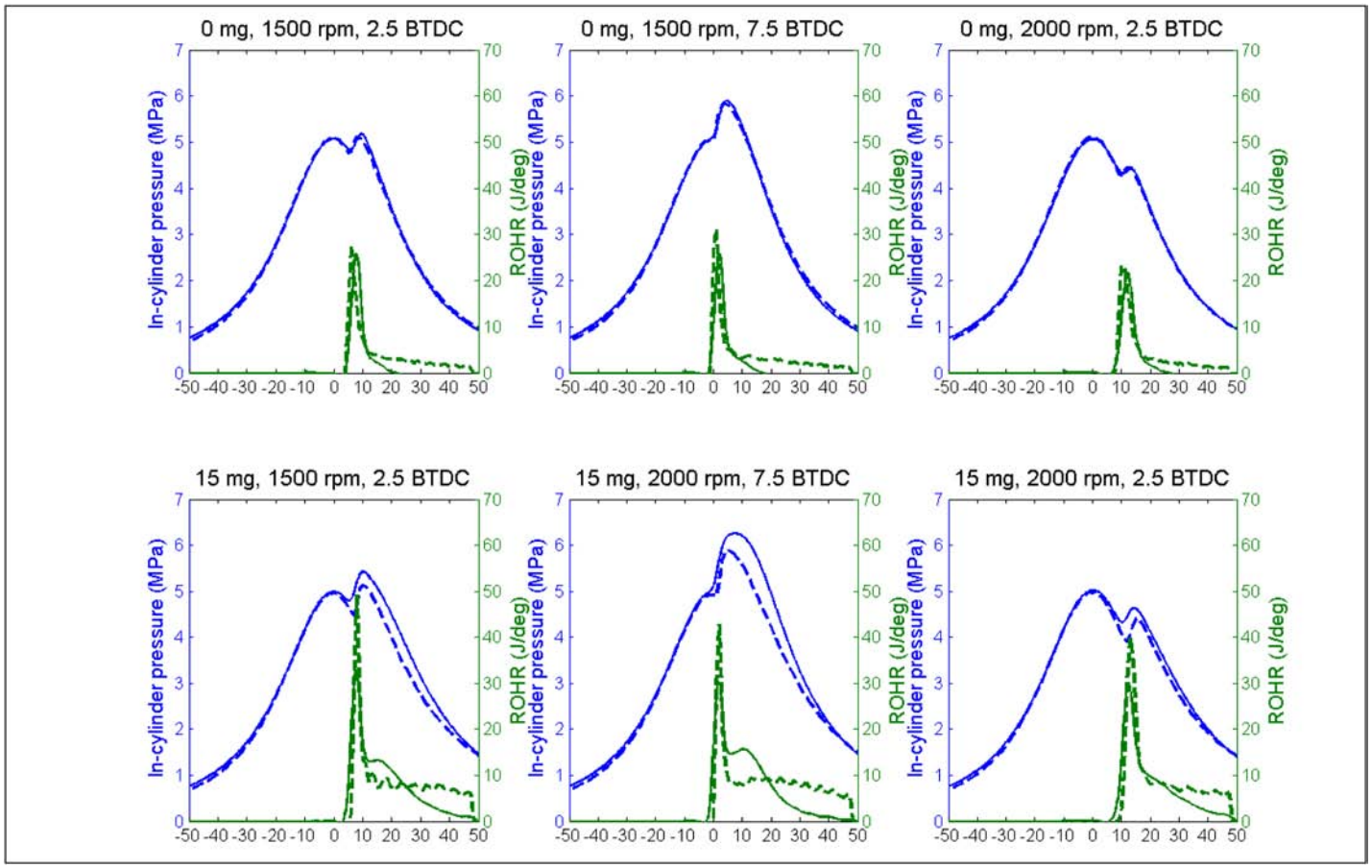

Figure 6. Traces of pressure and net ROHR for case 1 (—— exp. press. - - - num. press. —— exp. ROHR - - - num. ROHR)

giving an higher peak of ROHR in the premixed-combustion phase of diesel pilot. As far as emissions are concerned, the main trend of NO_x (Figure 7) and HC (Figure 8) are captured by the model.

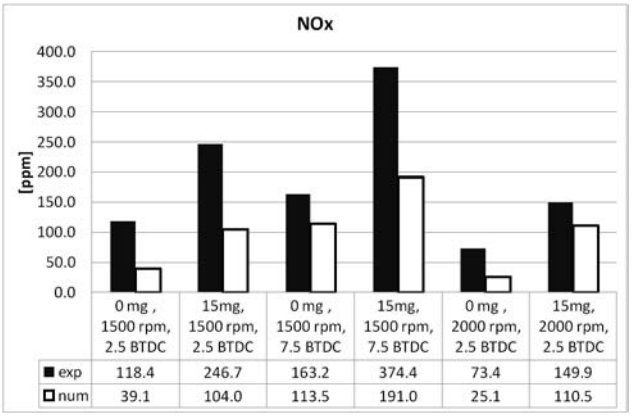

Figure 7. Emissions of NO_x for case 1

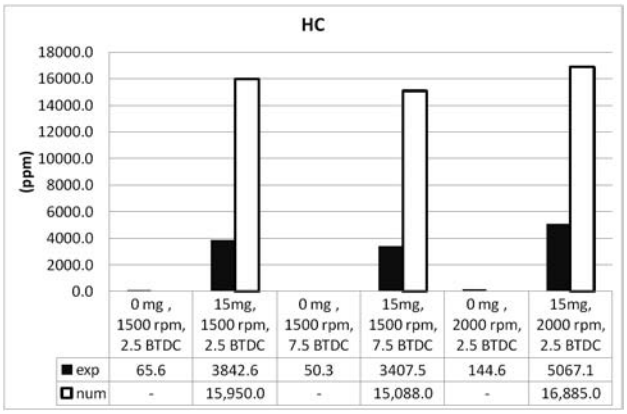

Figure 8. Emissions of HC for case 1

Case 2

The second set of tests (Table 3) considers the variation of mass per cycle of methane from 0 to 17.5mg while keeping the same engine speed (1500rpm) and pilot advance (7.5 BTDC). The pressure and ROHR traces are reported in Figure 9. In this case the peak of ROHR due to pilot combustion in the experimental case is only slightly influenced by the mass of CH4 while in the numerical case, the peak increases from 0 mg to 15mg. Also, the predicted heat release during the propagation phase of the flame persists in the expansion strokes while experimentally the propagation slows down faster. However, the emission trends

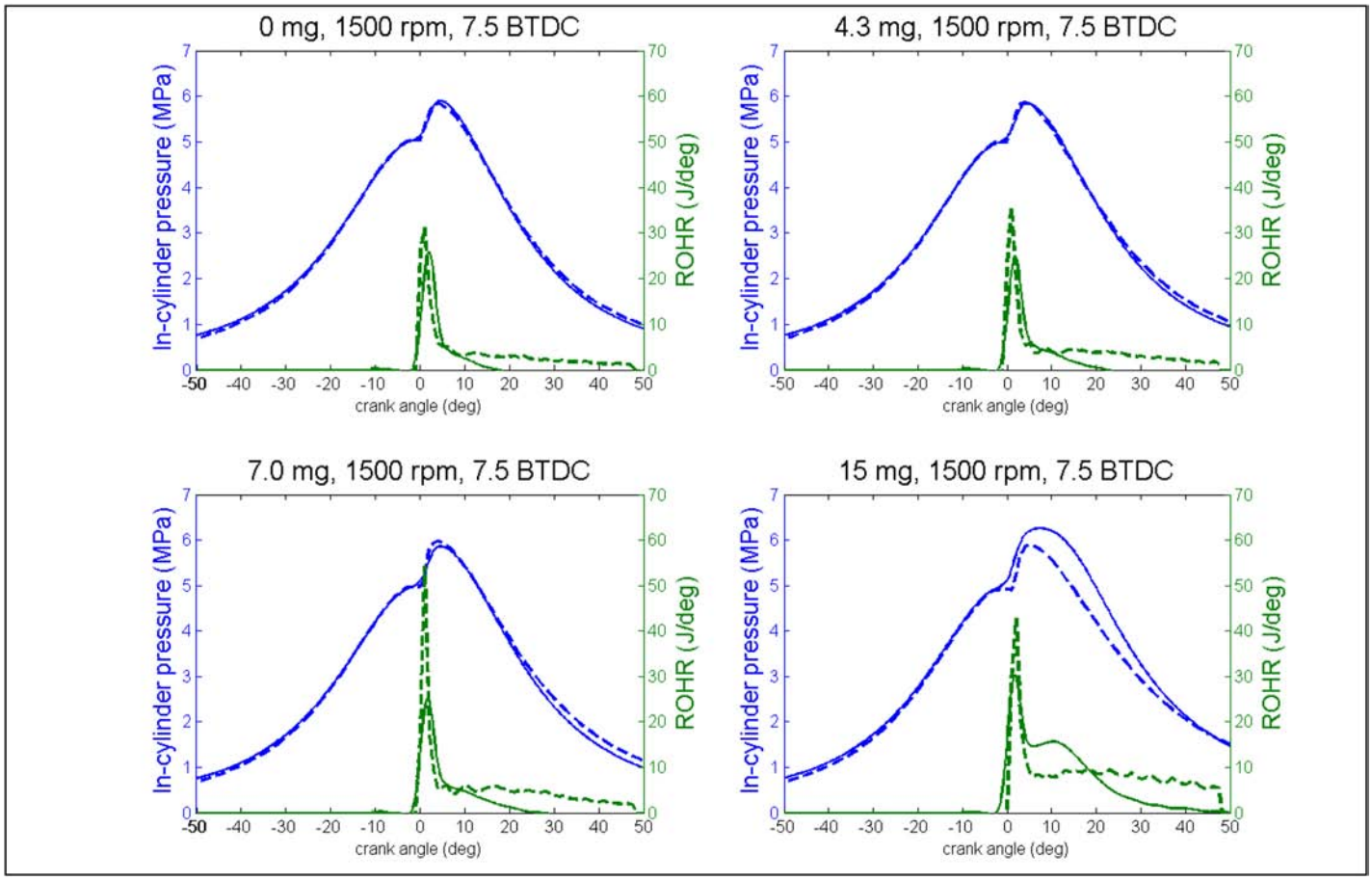

Figure 9. Pressure and net ROHR traces for case 2 —— exp. ROHR - - - num. ROHR)

are reasonably captured both in the case of NO_x (Figure 10) and HC (Figure 11).

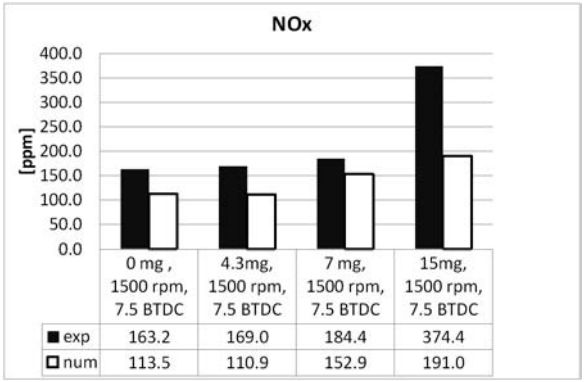

Figure 10. Emissions of NO_x for case 2

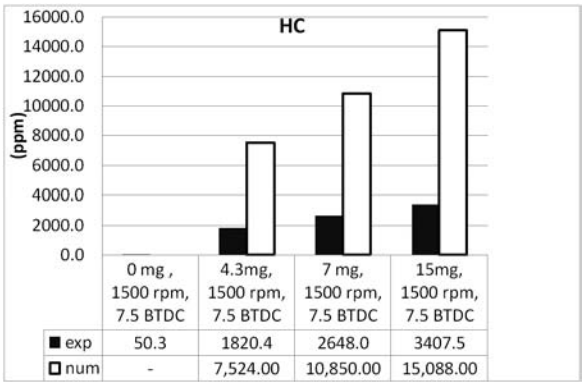

Figure 11. Emissions of HC for case 2

Discussion of the Validation

The numerical code with the proposed models appears to capture with accuracy compatible with the use of semi-empirical models, the effect of changing the engine speed and pilot advance quite well. Improvements have to be considered to the modeling of the methane combustions, in particular to the propagation of the flame. To this, the mapping of the turbulent flow field predicted with Fluent into the KIVA3V code will be considered.

The numerical values of emissions are quantitatively different from experimental data but the trends are well captured both

in case 1 (changing engine speed and pilot advance) and case 2 (changing mass of methane). All the test were performed without changing any value of the tuning parameters of Table 5.

The computational time required on the Linux cluster used for the validation (Beowulf system, master node Proliant DL180 G6, dual processor Xeon, 14 nodes Proliant DL160 G6 dual processor Xeon) is about 11 minutes for each test.

As a result, the model can be considered suitable for the combination with a multi-objective optimization of the bowl profile over different operating conditions.

DESIGN PROCEDURE

In a direct injection diesel, the combustion chamber includes the squish and the bowl regions shown in Figure 12. In order to reduce the compression ratio when converting the baseline engine from diesel to CNG combustion, it is possible to increase the volume of either the squish or the bowl.

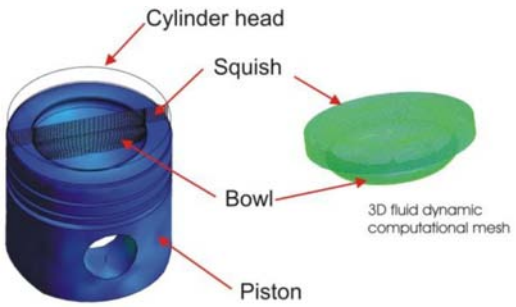

Figure 12. Nomenclature of the combustion chamber and its corresponding computational grid

The effect on the combustion processes obtained in the two cases can be quite different. For this reason, the proposed conversion procedure takes into account three possibilities:

- Changing only the squish volume;
- Changing only the bowl volume;
- Changing both squish and bowl volumes.

Moreover, if an offset is present in the original piston between the cylinder and the bowl axis (see Figure 13), the new chamber could have:

- No offset;
- The same offset of the original piston;
- Another offset value.

A design procedure has been proposed in a previous investigation for the conversion of a diesel engine to methane combustion. The procedure [6] consists of 5 steps:

STEP 1. definition of a database of combustion chambers that can be obtained from the original piston (Manufacturable Combustion Chambers MCCs);

STEP 2. selection of the chambers that are able to resist to the mechanical and thermal stresses expected in the CNG combustion process (Feasible Manufacturable Combustion Chambers FMCCs);

STEP 3. selection of the initial and boundary conditions and simulation of the combustion process with a multi-dimension simulation code;

STEP 4. analysis of the detonation behavior of the selected chamber (if required);

STEP 5. choice of the optimized combination of chamber configuration and design parameters (Optimized, Feasible and Manufacturable Combustion Chambers).

Steps 3 to 5 are performed in the framework of a multi-objective genetic algorithm optimization process. More details on the procedure and the design specification for either CNG-dedicated or dual fuel engines can be found in [6]

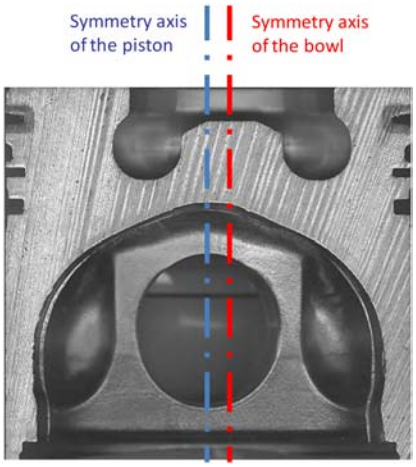

Figure 13. Combustion chamber with offset

A computational mesh is automatically generated for each combination of the parameters of Figure 14 is obtained with the Meshmaker tool. The mesh is represented by a sector of 72° domain with an average resolution of 2 mm (since a five-hole centrally located injector is used for diesel and the CH_4 is assumed to be uniformly distributed in the combustion chamber at the Intake Valve Closing).

The design method has been validated in a previous application to direct injection diesel engine [5, 24]. A Pareto optimal solution was selected after about 500 different combustion chamber designs.

A piston with the selected bowl was built and tested at operating conditions similar to those used in the optimization. The experimental results showed that the optimized chamber was effective in reducing soot and HC emissions and the measured reduction of soot was higher than the calculated one (up to 50% for one of the operating condition). As far as NO_x emissions are concerned, the experimental NO_x-soot

trade-off with increasing EGR agreed with the result of the optimization as shown in Figure 15 (see [24] for details).

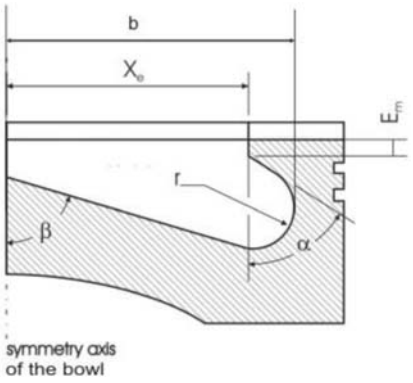

Figure 14. Parametric profile of the bowl

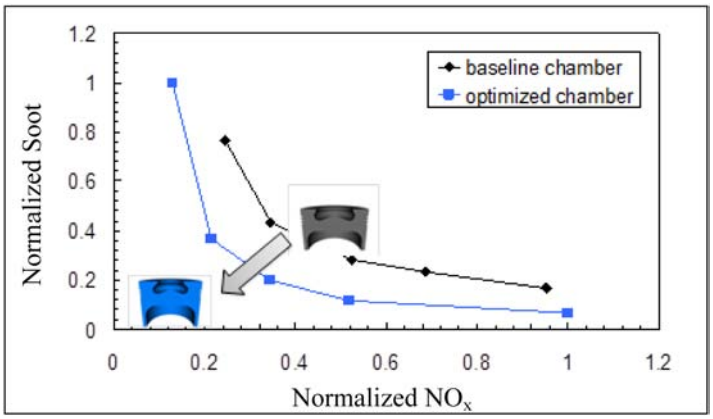

Figure 15. Experimental validation of the optimization process for a direct injection diesel engine (trade-off with increasing EGR)

EFFECT OF BOWL PROFILE

In a previous investigation, the design procedure has been applied over the same engine but with different operating conditions and a previous version of the combustion model [6]. Three different shapes of the bowl were identified and compared. Their specifications are reported in Table 6.

Table 6. Geometrical features of the selected chambers

Parameter	Unit	A	B	C
Xe	cm	1.7	1.7	2.4
α	deg	53	31	15
β	deg	53	49	56
r	cm	0.7	0.8	0.6
Em	cm	1.0	0.5	0.5
CR	-	17	17	17
SH	cm	0.153	0.153	0.153

The geometrical specification refers to the parameterization of the bowl profile shown in Figure 14 and based on five geometrical features named *Xe, Em, α, β* ed *r*. All the chambers have the same compression ratio (CR) and the same squish height (SH); thus, the have the same bowl volume. Details about the numerical procedure that define the final shape of the bowl and a selection of combustion chamber profiles generated for the reference engine can be found in [6].The maximum diameter of the bowl (*b*) in Figure 14 is not used for defining the bowl profile being the resultant of the choice of the bowl volume and the other parameters. However, it is used in the feasibility analysis.

The chambers have been compared over the same operating conditions used for the validation of the model (except those without CH_4). Figure 16 shows the results of the comparison in the case with 7 mg of Methane, 1500 rpm and pilot advance at 7.5 BTDC. Similar results were found in the other cases at 1500 rpm but are not reported here. Note that all the selected chambers guarantee an improvement of the combustion efficiency and consequently a reduction of HC emissions (see unburned CH_4 at 50 ATDC) and a quite complete elimination of soot emission. Unfortunately, the emissions of NO_x are quite higher than the baseline case. At 1500 rpm, Chamber A is best in terms of CH_4 conversion while chamber B and C guarantees the same levels of HC but with different levels of NO_x.

At 2000 rpm the behavior of the chambers is different. Chamber A and B are worse than baseline with respect to HC emissions (see unburned CH_4 at 50 ATDC) while the best results are obtained with chamber B. Once again the emissions of NO_x are worse than the baseline bowl for all the selected configurations.

The goal of the investigation is to present the combustion model and to check if the modification of the bowl profile can have a significant role in the conversion of an engine from diesel to methane. Thus, a detailed analysis of the combustion processes in the three chambers is not presented. However, the authors tried to separate the effect of the bowl profile on the combustion process due to pilot from that of methane. To this, the rate of heat release produced separately by the two fuels has been reported in Figure 18. In the case with early pilot (7.5°BTDC), low speed (1500 rpm) and very lean mixture (ER=0.18), changing the chamber profile determines an early combustion of the pilot but the peak of ROHR from diesel is the same for all chambers and equal to the baseline case (see the first row of Figure 18). The combustion of CH_4 starts early but the peak increases from baseline to chamber A.

If the equivalent ratio of the mixture is increased (see second row of Figure 18 with15 mg, 1500 rpm, 7.5 BTDC), the chambers show the same behavior than in the previous case as far as the ROHR due to methane combustion. The peak of ROHR from diesel is not only anticipated but also the highest for chamber A. Chamber B and C generated a similar combustion of the pilot in this operating condition.

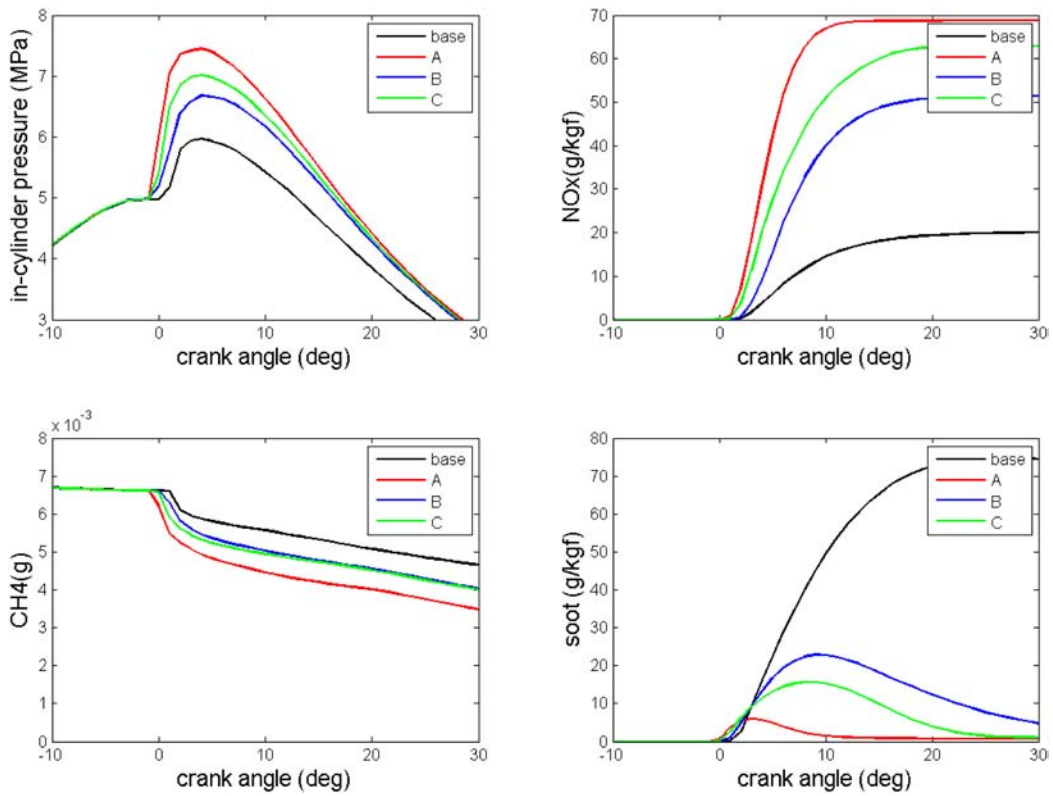

Figure 16. Comparison of the selected chambers (7 mg, 1500 rpm, 7.5 BTDC)

If the pilot is delayed (2.5 BTDC) with the same value of methane mass (15 mg) and engine speed (1500 rpm), the behavior of the chambers remains quite the same but chamber C gives a higher peak of diesel ROHR than chamber B (third row of Figure 18).

Finally, if the engine speed is increased (2000 rpm, 15 mg, 7.5BTDC), the combustion of CH_4 is consistent with the previous cases while the pilot ROHR obtained with each chamber is significantly different than in the case at 1500 rpm.

This analysis shows that, as far as the methane combustion is concerned, the optimization of the combustion chamber could be performed with respect to a single operating condition.

On the contrary, the combustion of the pilot obtained with each chambers is different when changing the operating conditions of the engine.

FEASIBILITY AND COST ANALYSIS

A correlation has been proposed to estimate the maximum temperature in the piston T_{max} and the maximum stress σ_{max} as a function of the chamber geometrical features:

$$T_{\max} = K_1 \cdot T_{bulk} \cdot \frac{V}{S} \tag{3}$$

$$\sigma_{\max} = K_2 \cdot p_{\max} \cdot \sqrt{b} \cdot \left(sen^2\alpha + \frac{K_3}{E_m} \right) \tag{4}$$

Where:

T_{bulk} is the maximum fluid temperature on the bowl surface;

V and S are, respectively, the volume and surface area of the bowl;

P_{max} is the maximum fluid temperature on the bowl surface;

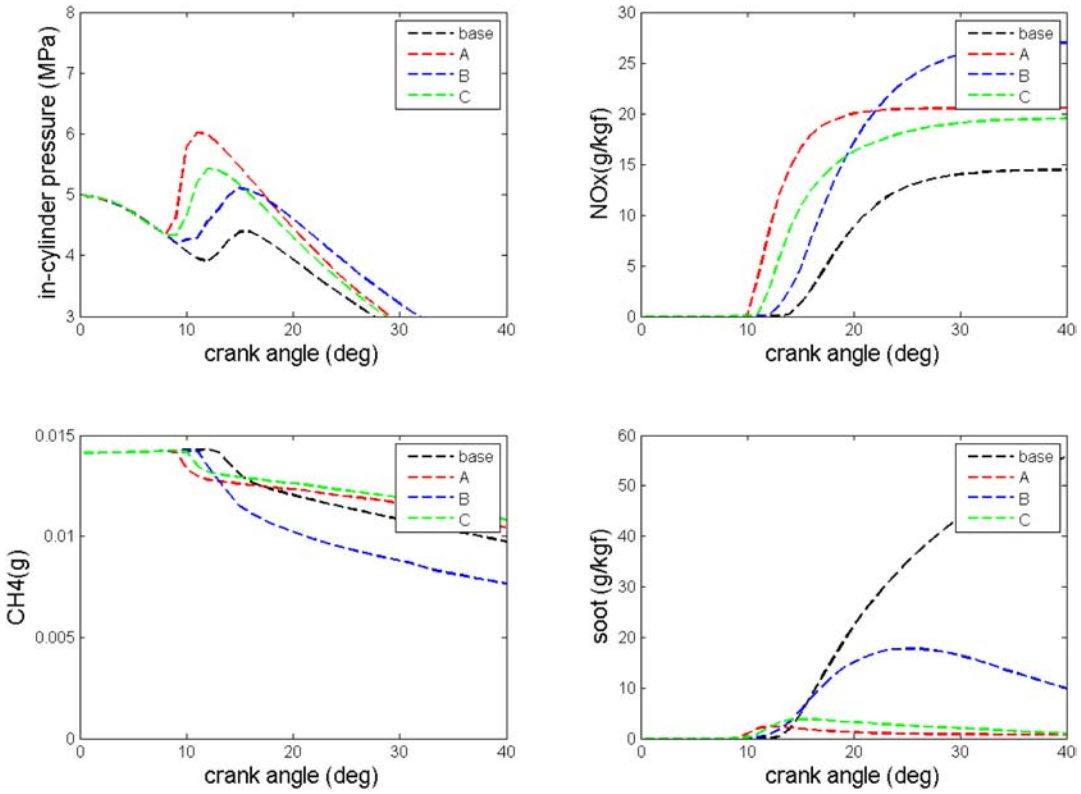

Figure 17. Comparison of the selected chambers (15 mg, 2000 rpm, 2.5 BTDC)

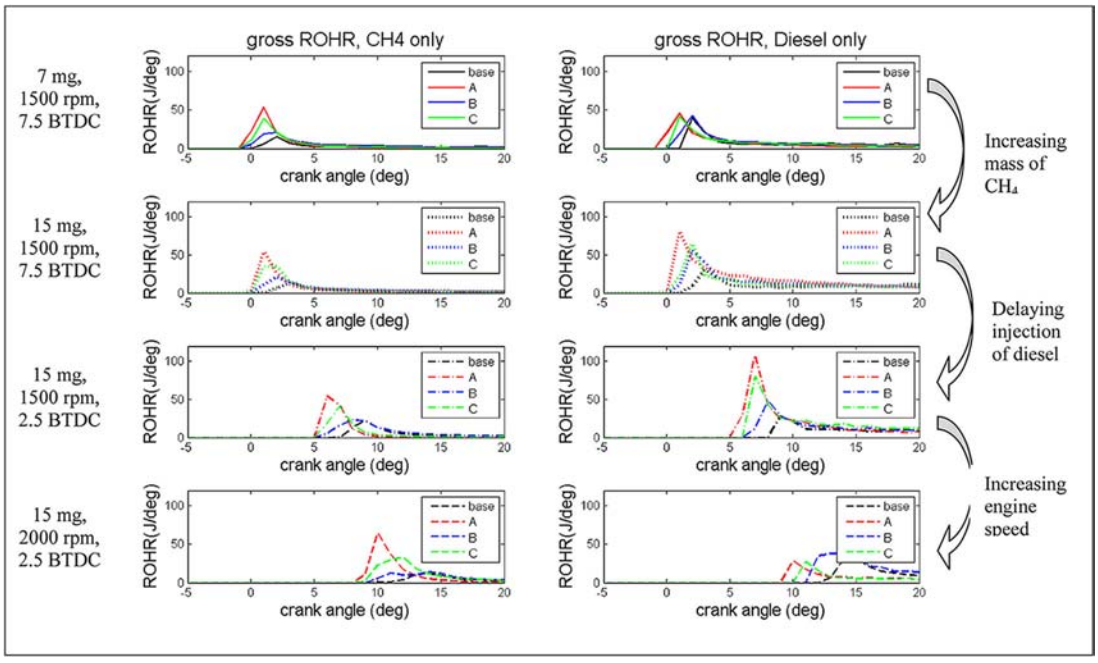

Figure 18. Effect of bowl profile on ROHR

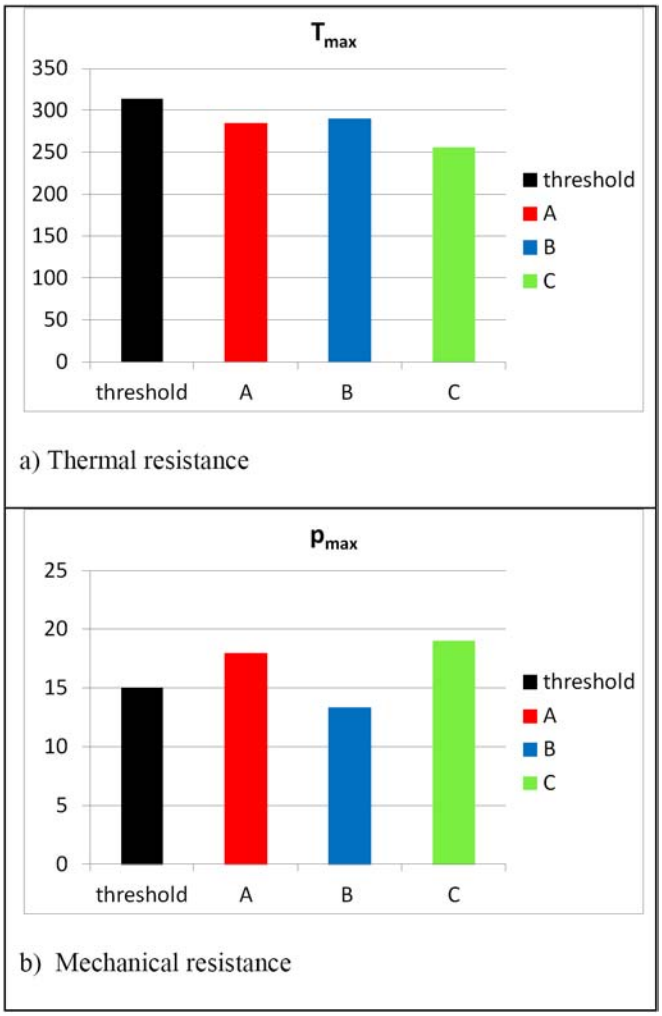

Figure 19. Mechanical analysis of the bowls

Note that "*b*" is the results of an iterative procedure implemented in Meshmaker [5] that changes its value until the pre-fixed bowl volume is guaranteed with the values chosen for the five parameters named *Xe, Em, α, β* ed *r*. Thus, all the geometrical features of the bowl have an indirect effect on the strength of the piston through the "*b*" parameter.

The values of the parameters K1, K2 and K3 have been obtained as a results of the application of the numerical procedure described in [23]. The empirical correlations have been applied to chamber A, B and C in Figure 19. To guarantee the mechanical resistance of the combustion chamber, threshold values of 315°C for T_{max} and 15 MPa and σ_{max} were considered. Note that chamber A and C satisfies the limit of 315 °C for the maximum temperature but not the threshold value for the pressure (15MPa). This means that the choice of these chambers would require the design of a new piston and a detailed analysis of the thermal and mechanical stresses. On the contrary, the adoption of chamber B could be done without much concern about the thermal stresses since both T_{max} and P_{max} are below the threshold values. This analysis was performed to stress the importance of taking into account the mechanical resistance of the piston in the optimization of the combustion bowl.

None of the combustion chambers found in the optimization satisfied the manufacturability test, i.e. the possibility to obtain the new chamber from the original piston as illustrated in Figure 20 where the blue is the original profile of the piston while the magenta dotted line represents the maximum theoretical area that can be occupied by the bowl. The automated procedure implemented in Matlab colors the profile of the piston in green if it is all contained inside the original piston. Points that are not compatible with the original pistons are shown in red. Note that the profile of Chamber C (also shown in Figure 20) is quite similar to the original piston. A bowl with the main geometrical specification of Chamber C but with a slightly higher volume could be obtained by cutting the re-entrance of the original piston (and modifying the shape of the central protrusion).

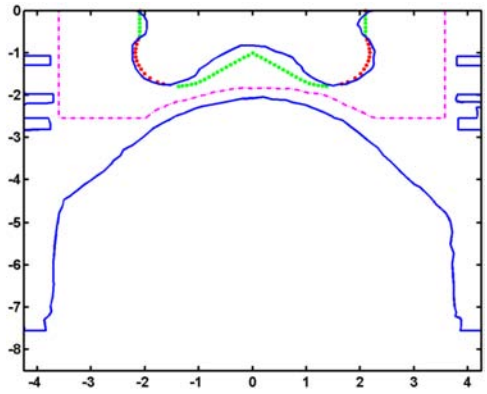

Figure 20. Profile of chamber C compared with the original piston (blue line)

SUMMARY AND CONCLUSIONS

A combustion model for dual fuel engines have been implemented in the Kiva3v code. The model is based on the characteristic time combustion model but it also can take into account the propagation of the flame with the level set method. The propagation of the flame, however, was not taken into account in the present investigation. Coupled with improved models for ignition and spray modeling, the dual fuel combustion model was found to reasonably capture the combustion processes and the emissions trend of a diesel-CH_4 engine when changing pilot advance, engine speed and methane equivalence ratio.

The model was used to analyze the effect of the bowl shape on dual fuel combustion. Three shapes of the bowl (all with the same volume) were compared with the original engine piston (baseline). The bowls were able to significanlty reduce the emissions of HC but with higher NOx emissions compared with the baseline combustion chamber. A multi-objective optimization will be performed as future development to look for a bowl able to reduce HC emissions without increasing NOx significantly. The bowls were also analyzed from a mechanical and conversion cost point of view.

The results of the analysis that the effect of bowl on CH_4 combustion is not influenced by engine speed, pilot advance and equivalence ratio but pilot combustion does. Therefore, the multi-objective optimization will be performed with respect to different engine speeds and diesel/methane energy ratio. Finally, some of the bowl profile found with the method will be built and test for a further validation of both the combustion model and the optimization procedure.

REFERENCES

1. Chandra R, Vijay V K, Subbarao P M V, Khura T K., "Performance evaluation of a constant speed IC engine on CNG, methane enriched biogas and biogas", *Applied Energy*; 88:3969-77, 2011.

2. Von Mitzlaff K., *Engines for biogas*, Friedr. Vieweg & Sohn Verlagsgesellschaft GmbH, 1988.

3. Sen A K, Wang J, Huang Z., "Investigating the effect of hydrogen addition on cyclic variability in a natural gas spark ignition engine: Wavelet multiresolution analysis", *Applied Energy*; 88:4860-6, 2011.

4. Namasivayam A M, Korakianitis T, Crookes R J, Bob-Manuel K D H, Olsen J., "Biodiesel, emulsified biodiesel and dimethyl ether as pilot fuels for natural gas fuelled engines", *Applied Energy*, 87: 769-78, 2010.

5. Donateo T. Optimal Design of a Common Rail Diesel Engine Piston, in Expensive Optimization Problems. In: Tenne Y, Goh C-K, editors. Adaptation, Learning, and Optimization. Springer Verlag; 2010, 2: p.513-41.

6. Donateo T., Tornese F., Laforgia D, "Computer-aided conversion of an engine from diesel to methane", Applied energy, in printing.

7. Karim G A., "Combustion in gas fueled compression: ignition engines of the dual fuel type", *Journal of Engineering for Gas Turbines and Power*, 125:827-36, 2003.

8. Karim, G., Liu, Z., and Jones, W., "Exhaust Emissions from Dual Fuel Engines at Light Load," SAE Technical Paper 932822, 1993, doi:10.4271/932822.

9. Singh, S., Kong, S., Reitz, R., Krishnan, S. et al., "Modeling and Experiments of Dual-Fuel Engine Combustion and Emissions," SAE Technical Paper 2004-01-0092, 2004, doi:10.4271/2004-01-0092.

10. Cordiner, S., Rocco, V., Scarcelli, R., Gambino, M. et al., "Experiments and Multi-Dimensional Simulation of Dual-Fuel Diesel/Natural Gas Engines," SAE Technical Paper 2007-24-0124, 2007, doi:10.4271/2007-24-0124.

11. Tan Z, Reitz R D., "An ignition and combustion model based on the level-set method for spark ignition engine multidimensional modeling", *Combustion and Flame*, 145:1-15, 2006.

12. Peters N. "Turbulent Combustion", Cambridge University Press; 2000.

13. de Risi, A., Zurlo, S., Donateo, T., and Laforgia, D., "3D Simulations And Experimental Validation of High EGR - PHCCI Combustion," SAE Technical Paper 2007-24-0037, 2007, doi:10.4271/2007-24-0037.

14. de Risi A, Donateo T, Laforgia D. "Theoretical Investigation on Variable Density Sprays", *Atomization and Sprays*, 12:329-58, 2002.

15. de Risi A, Donateo T, Laforgia D., "CFD Modeling of pilot injection and EGR in DI diesel engines", Proceedings of the 2004 Fall Technical Conference of the ASME Internal Combustion Engine Division, 251-63, 2004.

16. Carlucci A P, Laforgia D, Saracino R, Toto G., "Combustion and emission control in diesel-methane dual fuel engines: The effects of methane supply method combined with variable in-cylinder charge bulk motion", *Energy Conversion and Management* 52:3004-17, 2011.

17. Fu G, Zhao C, Liu B, Zhang F, Pang S, Li Y. "Investigation on the combustion characteristics of a diesel engine fueled with diesel-azides blends", *Applied Energy*, 91:98-102, 2012.

18. de Risi A, Donateo T, Laforgia D., "Theoretical investigation on the influence of physical parameters on soot and NOx engine emissions", Proceedings of the 2001 Spring Technical Conference of the ASME Internal Combustion Engine Division; 29 April - 2 May 2001; 36: 53-64, 2001.

19. Heywood J B., *Internal Combustion Engine Fundamentals*, New York, McGraw-Hill, 1988.

20. Wu H-W, Wu Z-Y,. Using Taguchi method on combustion performance of a diesel engine with diesel/ biodiesel blend and port-inducting H_2. Applied Energy 104:362, 2013;

21. Mavropoulos G C., "Experimental study of the interactions between long and short-term unsteady heat transfer responses on the in-cylinder and exhaust manifold diesel engine surfaces", *Applied Energy*; 88: 867-81, 2011.

22. Carrozza R, Donateo T, Laforgia D., "Effect of the combustion chamber profile on the in-cylinder flow field in a direction injection diesel engine", Proceedings of 61° Congresso Nazionale A.T.I., Perugia 12-15 September 2006.

23. de Risi A, Donateo T, Nobile F, Vadacca G, Vedruccio D. "Fluid Dynamics and Structural Behavior of Optimized Combustion Chamber Profiles", International Conference on CAE and Computational Technologies for Industry, 16-17 October 2008, Mestre Italy, 2008.

24. de Risi A, Donateo T, Laforgia D., "An Innovative Methodology to Improve the Design and the Performance of Direct Injection Diesel Engines", *International Journal of Engine Research*, 5:425-41, 2004.

DEFINITIONS/ABBREVIATIONS

ATDC - After Top Dead Center

BTDC - Before Top Dead Center

CI - Compression Ignition

CFD - Computational Fluid Dynamics

CNG - Compressed Natural Gas
CR - Compression ratio
ER - Equivalence Ratio
IVC - Intake Valve Closing
ROHR - Rate of Heat Release

The Engineering Meetings Board has approved this paper for publication. It has successfully completed SAE's peer review process under the supervision of the session organizer. This process requires a minimum of three (3) reviews by industry experts.

ISSN 0148-7191

SAE Customer Service:
Tel: 877-606-7323 (inside USA and Canada)
Tel: 724-776-4970 (outside USA)
Fax: 724-776-0790
Email: CustomerService@sae.org
SAE Web Address: http://www.sae.org
Printed in USA